Spin and Hyperfine Structure of Arsenic-76†*

R. L. CHRISTENSEN,‡ D. R. HAMILTON, H. G. BENNEWITZ,§ J. B. REYNOLDS,‖ AND H. H. STROKE¶
Palmer Physical Laboratory, Princeton University, Princeton, New Jersey

(Received January 13, 1961)

Hyperfine structure in the $^4S_{\frac{3}{2}}$ ground state of the radioactive atom As^{76} has been investigated by the method of magnetic resonance in an atomic beam produced by microwave discharge dissociation of arsenic vapor. $\Delta F=0$ resonances were observed within both the $F=\frac{5}{2}$ and $F=\frac{7}{2}$ atomic levels at several values of magnetic field up to about 5 oe, indicating that the spin of the As^{76} nucleus is 2. An analysis of multiple quantum transition spectra within the same F states gave a measurement for two of the hfs intervals: $\Delta\nu_{7/2,\frac{5}{2}}=\pm(117\pm4)$ Mc/sec and $\Delta\nu_{\frac{5}{2},\frac{3}{2}}=\pm(69\pm16)$ Mc/sec, with the same sign for both. From the value of the hfs constant A, the magnitude of the magnetic field at the arsenic nucleus is $(1.33\pm0.15)\times10^5$ oe in reasonable agreement with the variation in this field among similar atoms. The value of g_J has been found to be 1.994 ± 0.003 for arsenic.

INTRODUCTION

As part of a continuing program to determine the spins and moments of various radioactive nuclei, particularly the odd-odd nuclei, we have investigated the hyperfine structure (hfs) in the atomic ground state of 27-hr As^{76}. The technique employed was atomic beam magnetic resonance[1] with heavy emphasis placed on investigation of multiple quantum transitions which facilitated identification of resonances and, because of the larger associated high-field moment change, permitted better use to be made of the atom-optics in the machine. Measurements of the spin of As^{76} have been reported briefly by us,[2] using this technique, and by Pipkin and Culvahouse,[3] using double resonance techniques in arsenic-doped silicon. The experiment of these latter authors also gave the magnetic moment of this nucleus, as well as the hfs separation of the $^2S_{\frac{1}{2}}$ ground state for the donor arsenic atom in the silicon lattice.

We report here on the details of our determination of the spin and on the extension of this experiment to include the measurement of the hfs interaction constants in the free atom, whose ground state[4] (in the LS coupling approximation) is $^4S_{\frac{3}{2}}$. The measurement of the magnetic dipole interaction constant A leads to a value of the magnitude of the magnetic field at the arsenic nucleus, when use is made of the As^{76} nuclear dipole moment. Unfortunately, the precision attained in the measurement here reported of the quadrupole constant B does not permit the drawing of conclusions about the nuclear quadrupole moment of great significance. Our results do, however, indicate a value for the g_J value of the free arsenic atom.

TECHNIQUE AND PROCEDURE

The measurements here reported were made using the atomic beam magnetic resonance apparatus with six-pole focusing magnets which has previously been described.[5] Among the modifications to this machine, as described below, a lengthened C magnet (25 cm vs the 5 cm of the original) had been installed. This permitted the observation of a narrower (25 kc/sec vs 200 kc/sec) resonance line, due to the improved homogeneity of the static magnetic field.

The value of the static field was determined by the occasional observation of resonances in an atomic beam of K^{39} produced by an auxiliary oven and detected by the usual hot-wire detector. This beam, in addition, was useful in calibrating the strength of the rf oscillating field H_0 for the purpose of analysis of the multiple quantum transition spectrum in arsenic, described later. Values of rf magnetic field strength up to about 0.1 oe, useful for such transitions, were produced from a Rohde and Schwarz type SMLR power signal generator, with output capability of about one watt. Frequencies were determined to the nearest hundred cps by a Hewlett-Packard 524B electronic counter.

Production and Detection of Atomic Beam of Arsenic

Arsenic in the vapor state exists primarily as the polymers As_2 and As_4, which are inappropriate for an atomic beam experiment; thus a method of dissociation is required. The method chosen, on the basis of an ap-

† Based in part on a thesis submitted in 1957 by one of the authors (R.L.C.) to the faculty of Princeton University in partial fulfillment of the requirements for the degree of Doctor of Philosophy.

* This work was supported by the U. S. Atomic Energy Commission and the Higgins Scientific Trust Fund. Further details may be found in Atomic Energy Commission Technical Report NYO-8016, by R. L. Christensen, August, 1957 (unpublished).

‡ General Electric Coffin and Swope Fellow, 1955–1957. Now at IBM Research Center, Yorktown, New York.

§ Visiting Deutsche Forschungsgemeinschaft Fellow, 1956–1957. Permanent address: University of Bonn, Bonn, Germany.

‖ Now at the Department of Physics, Washington University, St. Louis, Missouri.

¶ Now at the Department of Physics, Massachusetts Institute of Technology, Cambridge, Massachusetts.

[1] The fundamentals of the technique have been described in such books as N. F. Ramsey, *Molecular Beams* (Oxford University Press, New York, 1956).

[2] R. L. Christensen, H. G. Bennewitz, D. R. Hamilton, J. B. Reynolds, and H. H. Stroke, Phys. Rev. **107**, 633 (1957).

[3] F. M. Pipkin and J. W. Culvahouse, Phys. Rev. **106**, 1102 (1957); **109**, 1423 (1958).

[4] W. F. Meggers, A. G. Shenstone, and C. E. Moore, J. Research Natl. Bur. Standards **45**, 346 (1950).

[5] A. Lemonick, F. M. Pipkin, and D. R. Hamilton, Rev. Sci. Instr. **26**, 1112 (1955).

parently high resulting fractional dissociation and possible applicability to other elements, was a 3000-Mc/sec microwave discharge. This was similar to the system developed by the M.I.T. atomic beam group.[6]

This system consisted essentially of an open circuit of about $\frac{1}{4}$ in. gap length at the end of a coaxial transmission line which was bridged by a discharge tube containing arsenic vapor. A power level of about 50 w was generated by a QK-61 magnetron; the *S*-band coaxial plumbing was conventional[7] except for the right-angle bend, or inverted "tee," at the load end of the line. This was designed especially for the arsenic work where we require an elevated temperature (300–350°C) to obtain sufficient vapor pressure to support the discharge. Thus, the outer wall of the tee was of sufficient thickness to contain, in holes drilled parallel to the axes of the transmission line and atomic beam machine, several molybdenum spiral heaters. The arsenic sample (about 200 mg) was contained in an 8-×0.6-cm diam quartz tube, sealed at one end and with a 0.07-cm orifice drawn at the other, or "snout," end. Because the central conductor of the tee was drilled through, this tube could be inserted from the back and positioned with the snout protruding slightly from the front of the tee. Care was taken that the arsenic crystals were located at the back of the tube to preclude their being strongly heated by the discharge.

After high enough temperature was attained in the tee, the discharge was initiated by application of a spark coil to a lead running down to the vicinity of the snout. This lead was also useful as a probe to sample the charged particle flux while the discharge was running and so to provide an indication of discharge stability. After breakdown, the tee assembly was moved slightly, over greased O rings, to locate the orifice directly in front of the circular stop at the entrance to the *A* magnet. This was verified by looking down the axis of the machine, from detector to source ends, with a telescope permanently aligned with the machine axis. After the initial adjustments, resonance experiments were performed in the usual way and as described below, until the arsenic charge was exhausted (some 10 hr).

In an auxiliary experiment an approximate value was measured for the fractional dissociation effected by the microwave discharge. This was a form of Stern-Gerlach experiment in which the atoms, by virtue of their possessing magnetic moments of the order of Bohr magnetons, were deflected, or focused, and the molecules were not. Similar experiments on other elements have been performed by others.[8] We used a permanent, six-pole focusing magnet[9] of length 11 cm, gap diameter 0.3 cm, and pole-tip field strength 8000 oe. The dissociation was determined from the comparison of relative beam intensities at an axial point at the exit from the magnet, when the magnet was, effectively, turned "on" or "off." This was done by moving the magnet on or off the beam axis; in the latter position a dummy brass tube reproduced the magnet dimensions in so far as the beam was concerned. These measurements indicated a fractional dissociation (ratio of number of atoms to number of atoms plus molecules) of 0.25 with a probable error of 0.13.

The radioactive As^{76} was produced by neutron irradiation of the single stable isotope, As^{75}, in the Brookhaven reactor. The container during this process was the same quartz tube (with the orifice temporarily closed with aluminum foil) subsequently used as the discharge tube, which facilitated handling of the hot samples. The initial strength of each sample was about 40 Mc. Sample purity was assured by using arsenic of 99.99% (supplier's spectroscopic value) purity. The decay rates of the radioactivity on a number of beam targets, described below, were found to be pure with a half-life of 26.3±0.1 hr, which compares favorably with the average reported value[10] of $26\frac{1}{2}$ hr for this nuclide.

Radioactive beam detection was performed in the usual manner of deposition followed by counting. The substrate was copper which had been cleaned mechanically and by solvents, although such treatment was not obviously necessary. It was found, however, that the collection efficiency (i.e., sticking probability) was temperature-dependent above about −90°C; it was vanishingly small at room temperature. Therefore, the copper disk was maintained at a temperature below −140°C during exposure to the beam. This cooling was effected by clamping the disk to an auxiliary, "backing" disk which in turn was firmly pressed against a cold trap charged with liquid nitrogen. The purpose of the auxiliary disk was to prevent the contamination of the detector disk with the stray arsenic with which the trap became coated over the course of a run.

The intensity of the beam was determined by removing the substrates from the vacuum, and sealing them in a matrix of moisture-absorbing paper with Scotch tape. They were then mounted on holders and placed next to 2π scintillation β counters with conventional electronics, as previously described.[11]

Beam Fluctuations and the Rotating-Disk "Flop-Out" Procedure

The beam of arsenic atoms produced by the microwave discharge was seldom as steady as required to

[6] J. G. King and J. Zacharias, *Advances in Electronics and Electron Physics*, edited by L. Marton (Academic Press, Inc., New York, 1956), Vol. 8, p. 1.

[7] G. L. Ragan, *Microwave Transmission Circuits* (McGraw-Hill Book Company, Inc., New York, 1948).

[8] J. M. Hendrie, J. Chem. Phys. **22**, 1503 (1954); B. Bederson, H. Malamud, and J. Hammer, Bull. Am. Phys. Soc. **2**, 172 (1957).

[9] R. L. Christensen and D. R. Hamilton, Rev. Sci. Instr. **30**, 356 (1959).

[10] D. Strominger, J. M. Hollander, and G. T. Seaborg, Revs. Modern Phys. **30**, 585 (1958).

[11] J. B. Reynolds, R. L. Christensen, D. R. Hamilton, W. M. Hooke, and H. H. Stroke, Phys. Rev. **109**, 465 (1958).

permit taking runs in the customary fashion. That would entail exposing successive collector disks one at a time, each for a period of about five minutes.[12] Thus, stability would be required for about an hour to complete a run of about eight datum points.

However, an averaging scheme was devised whereby the discharge fluctuations affected each exposed substrate to approximately the same degree; this was based on converting the machine from flop-in to flop-out operation. At the plane of detection in this focusing machine, i.e., immediately after the B magnet, those atoms which have undergone an rf-induced transition are located within an annulus between diameters of 0.3 and 1.0 in. The unflopped atoms are, by and large, focused to a small region of about $\frac{1}{4}$ in. diameter on the axis. A resonance may therefore be observed either as an increase in atoms deposited in the former region (flop-in) or as a decrease at the latter position (flop-out). Stops can be suitably arranged so that only one portion is detected.

The advantage of the flop-out technique (which, in this experiment, overweighed the usual disadvantage of inherently lower signal-to-noise ratio) arose from the smaller substrate required for beam detection. This permitted dividing the $1\frac{3}{4}$-in. diam copper disk into eight sectors and offsetting the disk holder slightly ($\frac{9}{16}$ in.) from the machine axis so one sector at a time could be rotated onto that axis for beam condensation purposes. This permitted the frequent change at fixed time intervals from sector to sector, with each of which was associated a particular rf frequency applied to the transition region (including two sectors for which no rf field was used, for beam normalization). In this way the radioactive condensate was accumulated to the desired level in many small increments. A typical schedule called for 20-sec exposures and 15 rotations of the disk, thereby providing 5-min exposure for each sector over a total elapsed time of about an hour. The exposure of any particular sector many times and only shortly after that of any other provided the desired averaging. The application of this technique in the case of short-lived atoms effusing from ovens whose temperature was inconstant has been described elsewhere.[11]

HYPERFINE STRUCTURE ENERGY LEVELS FOR $J=\frac{3}{2}$, $I=2$

Hyperfine structure interaction energy in an atom, caused by the electromagnetic interaction between nucleus and electrons, can be expressed as a sum of magnetic dipole, electric quadrupole, magnetic octupole, etc. contributions.[1,13] To sufficient exactness for this experiment, only the first two terms need be considered, such refinements as hfs anomalies are neglected, and other atomic energy levels are far enough removed from the ground state ($^4S_{\frac{3}{2}}$) to be ignored in our analysis.

Under these conditions, the hfs energy levels at zero external field are describable in terms of the nuclear spin I, the atomic quantum number J, and the hfs constants A and B, which are given by

$$A=-\frac{1}{h}\frac{\mu_I}{I}\frac{H(0)}{J}, \tag{1}$$

and

$$B=eqQ/h. \tag{2}$$

In these equations, $H(0)$ is the magnetic field produced at the nucleus by the electrons, q is the z component of the electric field gradient so produced, and Q is the nuclear quadrupole moment. The other symbols have their usual meanings. One of the interesting results of the present experiment is the deduction of a value of $H(0)$ for As and the comparison of the value with those for other elements in the same group of the periodic table.

For a given atom, the zero-field energy levels depend only on the total angular momentum quantum number F, and not on its z component m; hence, the levels are $(2F+1)$-fold degenerate. For an atom with $J=\frac{3}{2}$ and $I=2$, such as As^{76}, these levels are given by

$$\begin{aligned} E_{7/2}&=3hA+\tfrac{1}{4}hB,\\ E_{5/2}&=-\tfrac{1}{2}hA-\tfrac{5}{8}hB,\\ E_{3/2}&=-3hA,\\ E_{1/2}&=-(9/2)hA+(7/8)hB, \end{aligned} \tag{3}$$

where the subscripts indicate the possible values of F which derive from these values of J and I. Our experiment deals with the magnetic sublevels of the first two levels and with the two intervals between the first three levels. Application of an external magnetic field (static, or "C" field), assumed to define the z direction, removes the degeneracy by adding the perturbation term to the Hamiltonian:

$$\mathcal{H}(\text{mag})=xhAJ_z, \tag{4}$$

where x is the customary dimensionless parameter indicating the strength of the C field:

$$x=g_J\mu_0 H_C/hA. \tag{5}$$

We have neglected a similar, but much smaller, term involving the nuclear g value, which, it turns out, is entirely satisfactory in these experiments.

The energy values corresponding to the various states may be determined in the usual fashion by solution of the secular equations. In general (and for the As^{76} atom) these will be of order higher than two and so recourse is customarily made to numerical methods and machine computation for exact solutions. However, another approach is to treat the external field as a perturbation on the zero-field levels; this is appropriate in the so-called Zeeman region.

[12] R. L. Christensen, D. R. Hamilton, A. Lemonick, F. M. Pipkin, J. B. Reynolds, and H. H. Stroke, Phys. Rev. **101**, 1389 (1956).

[13] H. Kopfermann, *Nuclear Moments* (Academic Press, Inc., New York, 1956), 2nd ed.

Sufficient accuracy for our purposes is provided by a perturbation calculation[14] carried to third order:

$$E'(F,m)=E'_F+Rmx+\left\{\frac{Q(F^2-m^2)}{E'_F-E'_{F-1}}-\frac{P[(F+1)^2-m^2]}{E'_{F+1}-E'_F}\right\}x^2+\left\{\frac{Q(F^2-m^2)}{(E'_F-E'_{F-1})^2(F-1)F(F+1)}-\frac{P[(F+1)^2-m^2]}{(E'_{F+1}-E'_F)^2F(F+1)(F+2)}\right\}\times[J(J+1)-I(I+1)]mx^3. \quad (6)$$

Here the prime indicates reduction to dimensionless form by division by hA. The first term on the right is given by Eq. (3). The functions P, Q (obviously not to be confused with nuclear quadrupole moment), and R are given by

$$P\equiv\frac{(F+1-J+I)(F+1+J-I)(J+I+F+2)(J+I-F)}{4(F+1)^2(2F+1)(2F+3)},$$

$$Q\equiv\frac{(F-J+I)(F+J-I)(J+I+1+F)(J+I+1-F)}{4F^2(2F-1)(2F+1)},$$

$$R\equiv\frac{J(J+1)-I(I+1)+F(F+1)}{2F(F+1)}. \quad (7)$$

Figure 1 shows the dependence of the hfs energy levels upon external field for an atom with $J=\frac{3}{2}$ and $I=2$. The region from $0\leq x\leq 1$ represents the results of an exact computer solution for the energy values to which the values given by Eq. (6) are an approximation. The points at $x=10$ are the result of a strong-field perturbation theory solution. The transition from the Zeeman region (where $x\ll 1$ and F, m are good quantum numbers) to the Back-Goudsmit region (where $x\gg 1$ and m_I, m_J, and $m=m_I+m_J$ are the good quantum numbers) is indicated schematically. Figure 1 is drawn for $A>0$, $B=0$; the corresponding diagram for $A<0$, $B=0$ can be obtained by reflecting the figure in a horizontal line and reversing the sign of the m, m_I, m_J quantum numbers associated with a given energy level line in the diagram.

This figure illustrates the fact that for $J=\frac{3}{2}$ there are, to first approximation, four different possible strong field moments as given by $\mu=-g_J m_J\mu_0$. It is also apparent from the figure, and is true for arbitrary I (as may be verified by using the relation $m=m_I+m_J$ to construct the connection between the Zeeman and Back-Goudsmit states), that only for the two largest

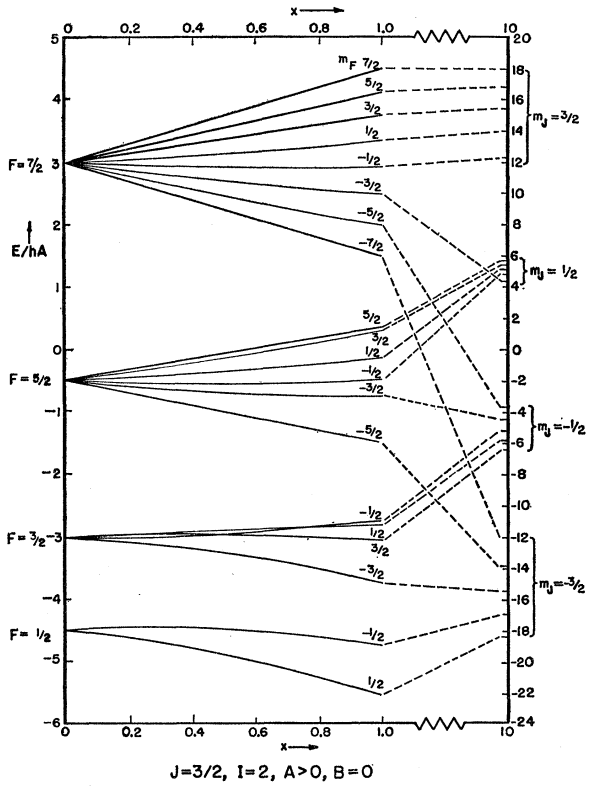

FIG. 1. Dimensionless hyperfine energy level diagram for an atom with $J=\frac{3}{2}$, $I=2$, $A>0$, and $B=0$. The magnetic field parameter x is given by $x=g_J\mu_0 H_C/hA$. The solid lines indicate the result of an exact computer solution; the dashed lines indicate schematically the transition to the values obtained by a high-field perturbation calculation at $x=10$. Note change of both vertical and horizontal scales between $x=1$ and 10.

values of F will any transitions with $\Delta F=0$ (to which we limit our attention throughout this paper) connect states with opposite signs of strong-field moment. In this apparatus only the states $m_J>0$ will be focused by the A magnet and enter the B magnet with appreciable intensity; a strong resonance is to be expected only when an atom in a state $m_J>0$ makes a transition to $m_J<0$. Thus at weak static fields ($x\ll 1$) resonances are to be expected for $\Delta F=0$ transitions at two frequencies which are linear in H_C and which correspond to $F=I+\frac{3}{2}$, $I+\frac{1}{2}$, as can be shown from Eq. (8) (below) carried only through the linear term.

Measurement of either or both of these frequencies, made at several values of H_C, determines I but not the intervals between zero-field levels. For the latter purpose, and short of going to $\Delta F=1$ transitions, one desires to go to a high enough x (i.e., static field) to observe nonlinearities in the dependence of frequency on field. But now one must live with, and if possible capitalize upon, the availability of multiple-quantum transitions,[15] of multiplicity N, for which $\Delta F=0$,

[14] We use the angular momentum commutation rules of E. U. Condon and G. H. Shortley, *Theory of Atomic Spectra* (Cambridge University Press, New York, 1935).

[15] M. N. Hack, Phys. Rev. **104**, 84 (1956).

$|\Delta m_F| \equiv N > 1$. From Eq. (6) the frequency ν_N corresponding to the energy difference in an N-quantum transition for arbitrary I and J is given by

$$\nu_N = Rg_J k \pm \left[\frac{P}{\Delta\nu_{F+1,F}} - \frac{Q}{\Delta\nu_{F,F-1}}\right](N+2m)(g_J k)^2 + \left[\frac{Q}{(\Delta\nu_{F,F-1})^2}\frac{F^2-3m^2-3mN-N^2}{(F-1)F(F+1)} - \frac{P}{(\Delta\nu_{F+1,F})^2}\frac{(F+1)^2-3m^2-3mN-N^2}{F(F+1)(F+2)}\right] \times [J(J+1)-I(I+1)](g_J k)^3. \quad (8)$$

To allow writing this as a single equation applicable to either sign of A (hence the $\pm$ on the quadratic term), the value of m which is to be used is selected by the following convention: If $A>0$, m is the quantum number which characterizes the final state in the N-quantum transition; for $A<0$, m is the negative of the m value for the initial level.

The linear term in this equation provides an important reference point in any given multiple-quantum spectrum and is denoted by

$$\nu_{\text{lin}} \equiv Rg_J k. \quad (9)$$

In the above we have defined

$$\Delta\nu_{F,F'} \equiv (E_F - E_{F'})/h, \quad (10)$$

and

$$k \equiv Ax/g_J = \mu_0 H_C/h. \quad (11)$$

It will be seen from Eq. (8) that the term in ν_N which is linear in k is independent of N, but that the nonlinear terms are dependent on both N and m. The multiple-quantum resonances cluster around ν_{lin} and are separated from each other by a spacing $\delta\nu$ which is given to

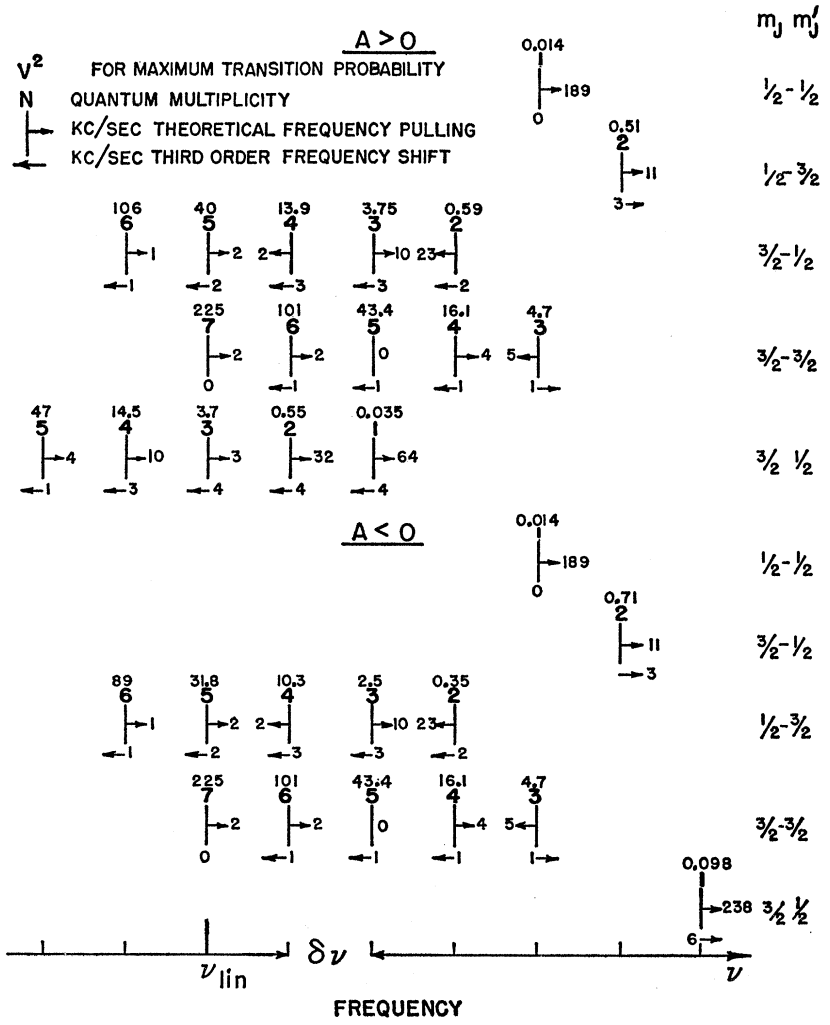

FIG. 2. Theoretical multiple quantum spectrum for $\Delta F=0$ transitions among $F=\frac{7}{2}$ levels of a $J=\frac{3}{2}$, $I=2$ atom. Abscissa indicates frequency separation, in units of $\delta\nu$ calculated to second order, between transitions; ordinate indicates initial and final values of m_J, and sign of A. The bold number over each transition is the multiplicity N. The significance of the other numbers is indicated by the key. They were calculated for the values of static field and of rf power parameter ($V^2=100$) actually used in the experimental runs of Fig. 6, and for early, approximate values of the hfs intervals.

terms cubic in x by the relation

$$\delta\nu \equiv \nu_N - \nu_{N+1}$$
$$= \pm\left\{\frac{Q}{\Delta\nu_{F,F-1}} - \frac{P}{\Delta\nu_{F+1,F}}\right\}(g_J k)^2$$
$$+\left\{\frac{Q}{(\Delta\nu_{F,F-1})^2}\frac{1}{(F-1)F(F+1)}\right.$$
$$\left.-\frac{P}{(\Delta\nu_{F+1,F})^2}\frac{1}{F(F+1)(F+2)}\right\}$$
$$\times[J(J+1)-I(I+1)](g_J k)^3[3m+2N+1], \quad (12)$$

where again the $\pm$ option corresponds to $A>0$ or $A<0$.

The second-order spectrum, whose spacing does not depend on m and N, of resonance frequencies for $I=2$, $J=\frac{3}{2}$ expected from these relations is displayed in Fig. 2 for $F=\frac{7}{2}$ and in Fig. 3 for $F=\frac{5}{2}$, together with further information which will be discussed shortly. It will be observed that: (a) the quantum multiplicity N is indicated for each transition and that the frequencies are grouped in accordance with the initial and final high-field quantum number values m_J and m'_J; (b) only positive initial m_J are listed which corresponds to the fact that atoms with negative m_J are defocused by the A magnet; (c) values are included corresponding to transitions between the states $m_J=\frac{3}{2}$ and $\frac{1}{2}$. This last action might be thought inappropriate from the point of view of atom optics in the machine. Thus, for example, $m_J=+\frac{3}{2}$ atoms are focused by the A magnet, but whether their likelihood of reaching the detector is increased or decreased by transition in the C field to a state $m_J=\frac{1}{2}$ is not apparent and undoubtedly differs from velocity to velocity; in any case, the possibility of observation of such a resonance needs to be taken into account.

The "third-order frequency shift" recorded in Figs. 2 and 3, calculated from Eq. (8), refers to the specific value of H_C or k to which the principal experimental data (Figs. 6 and 7) correspond, and further is calculated on the basis of approximate values for the $\Delta\nu$'s in the cited equation.

The "theoretical frequency pulling" indicated in Figs. 2 and 3 has been calculated under similar conditions by means of Hack's theory[15] of multiple-quantum transitions, and first-order wave functions. This pulling, which goes to zero in the limit of zero-order wave functions, is proportional to terms in the square of the matrix elements given in Eq. (14) below and to the square of the rf field strength.

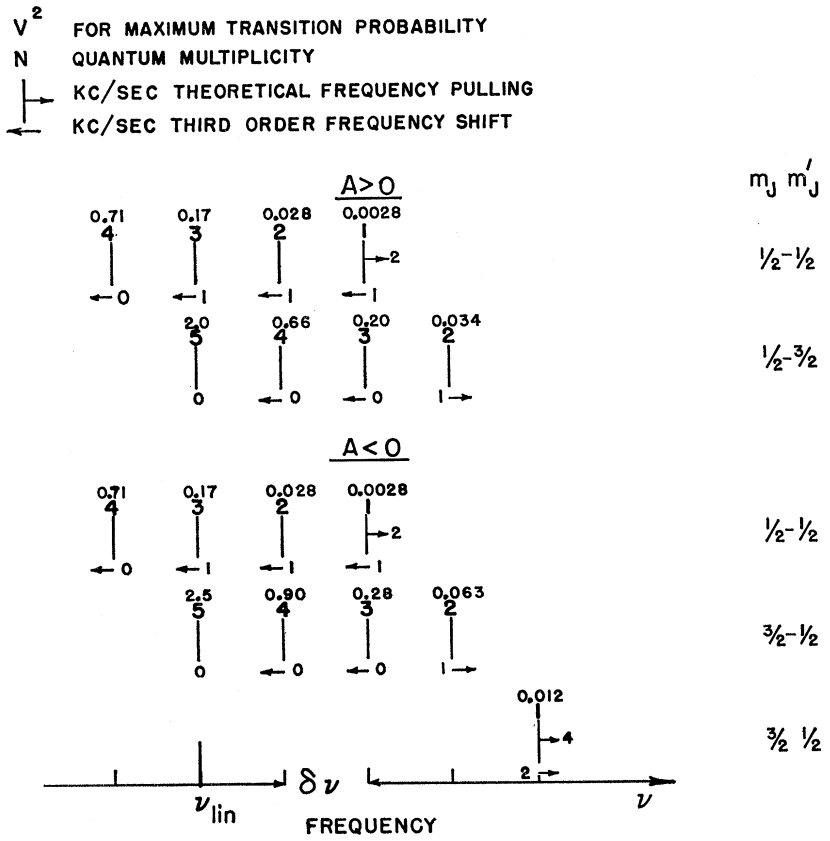

FIG. 3. Theoretical multiple quantum spectrum for $\Delta F=0$ transitions among $F=\frac{5}{2}$ levels of a $J=\frac{3}{2}, I=2$ atom. Otherwise similar to Fig. 3, except parameters here calculated for the values of static field and rf power ($V^2=0.115$) actually used in the runs of Fig. 7.

RADIO-FREQUENCY POWER REQUIREMENTS IN MULTIPLE-QUANTUM TRANSITIONS

As quantum multiplicity increases, the rf field required to produce the transition also increases. The interpretation of the multiple-quantum spectra observed in this work requires some knowledge of the transition probability associated with a given resonance at a given applied rf power; this will now be discussed, with particular reference to Hack's theory.[15]

At the frequency appropriate to maximizing a given N-quantum transition, the transition probability according to Hack (and in his notation) is equal to $\sin^2(t\,\delta)$. Here t is the time spent within the oscillating rf magnetic field, which has amplitude H_0. This field is assumed to drop abruptly to zero at the boundaries of the transition-inducing region.

The numerator of δ is the product of N matrix elements of the rf perturbation between the adjacent states lying between the initial and final states of the $\Delta F=0$, $|\Delta m|=N$ transition. The denominator of δ is a product of $(N-1)$ resonance (frequency difference) terms. Through the product of the resonance denominators, δ depends on the static magnetic field since this determines the departure from uniformity of the intermediate level spacings. This dependence on the static field is most easily expressed to first (and suitable) approximation in terms of the quantity $\delta\nu$, given by Eq. (12) and carried to second order. That is, it is sufficiently accurate here to use the approximation in which the multiple-quantum spectrum is one of uniform spacing. A straightforward calculation then yields

$$\delta=\left(\frac{g_J\mu_0 H_0}{4\hbar}\right)^N \frac{A'_{i,i-1}\cdots A'_{f+1,f}}{(2\pi\delta\nu)^{N-1}[(N-1)!]^2}, \tag{13}$$

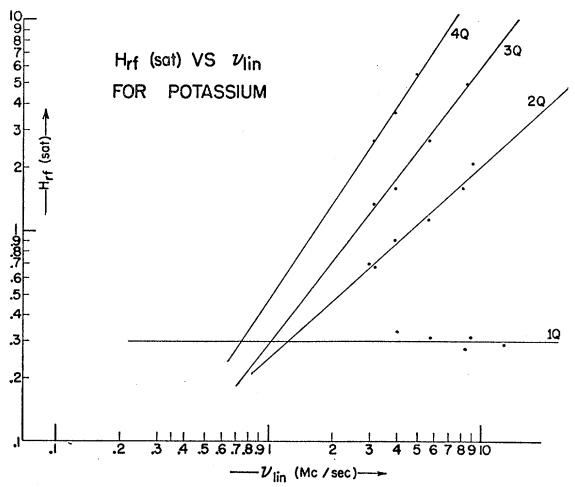

FIG. 4. Observed values of rf magnetic field, in arbitrary units (H_0 in text), which causes saturation of 1, 2, 3, or 4-quantum transition in K^{39}, as a function of the linear (in static field) term for the resonant frequency. The significance of the relative heights and slopes of the straight lines drawn through the empirical points is described in the text.

in which the initial $\cdots$ final states are denoted by subscripts i, $i-1\cdots f+1$, f. The normalized matrix elements are given by

$$A'_{ij}=\langle\psi_i|J_++J_-|\psi_j\rangle, \tag{14}$$

in which $J_\pm$ is the usual angular momentum operator $J_x\pm iJ_y$.

From Eq. (13) it will be noted that $\delta\propto H_0{}^N$ and so, for small values of H_0, i.e., for small values of $\sin^2(t\delta)$, the transition probability varies as $H_0{}^{2N}$. This dependence was used in earlier flop-in experiments[12] on Au^{198} and Au^{199} to determine the multiplicity of observed transitions. However, in the present flop-out experiments where the resonances were relatively small, it was necessary to attempt for some transitions to maximize the transition probability, i.e., to adjust H_0 so that the product $t\delta$ approximated $\frac{1}{2}\pi$; and for all transitions it was important to know the relation between applied and optimum rf power.

For t, we use the value given by the uncertainty principle: $t=1/\delta'\nu$, where $\delta'\nu$ is the intrinsic (i.e., exclusive of field inhomogeneity) linewidth of a single-quantum transition. The optimum value of rf field is then given by

$$H_0=\frac{2h}{g_J\mu_0}\{[(N-1)!]^2 2^{N-2}\}^{1/N} \times\left(\frac{\delta'\nu}{A'_{i,i-1}\cdots A'_{f+1,f}}\right)^{1/N}(\delta\nu)^{(N-1)/N}. \tag{15}$$

Before this expression could be used in the arsenic experiments a value of $\delta'\nu$ had to be obtained and some method of measuring H_0 devised. Auxiliary experiments with a beam of potassium atoms provided these tools as well as a verification of the general multiple-quantum relations here under discussion. The results of such experiments are shown in Fig. 4. By means of a pickup loop near the rf field and a calibrated almost-square-law crystal detector, H_0 was measured in arbitrary units and its optimum value determined for values of $\nu_{\rm lin}$ ranging from 3 to 10 Mc/sec. (At low frequencies the multiple-quantum peaks are not resolved; at higher frequencies the assumption of uniform spacing of multiple-quantum resonances becomes increasingly less valid.)

Both the slopes and the relative heights (i.e., intercepts of the two-, three-, and four-quantum lines with the one-quantum) are significant. Because $\delta\nu$ varies as the square of H_C, hence of $\nu_{\rm lin}$, Eq. (15) predicts that the slopes vary as $2(N-1)/N$ and should equal 0, 1, $\frac{4}{3}$, and $\frac{3}{2}$ for $N=1$, 2, 3, and 4, respectively. The observed slopes are 0, 0.91, 1.32, and 1.53 in the same order, in good agreement. The static-field independent optimum value of H_0 for $N=1$ also provides a means of converting the arbitrary units of the observed rf field parameter to absolute units. In turn, calculated absolute units for

arsenic can be related to this parameter. For example, Eq. (15), when the value of $\delta'\nu$ determined below was inserted, showed that 0.3 units of the ordinate in Fig. 4 corresponded to $H_0=0.01$ oe.

The values of ν_{lin} at which H_0 for the three multiple quantum transitions of Fig. 4 equal that for the single quantum can be used to determine $\delta'\nu$ for potassium. The ratio of the expressions [Eq. (15)] for H_0 for N quantum and for single quantum is set equal to 1. This equation is then solved for $\delta\nu$ (hence, ν_{lin}) in terms of $\delta'\nu$ and calculable matrix elements and the known hfs interval for K^{39}. The data of Fig. 4 show intercepts at values of ν_{lin} of 1.25, 1.03, and 0.75 Mc/sec for $N=2$, 3, and 4. A good fit to the data (1.36, 0.96, 0.72 Mc/sec, respectively) is provided by the indicated equation if we take $\delta'\nu=13$ kc/sec. This agrees well with an estimate provided by the most probable (kinetic theory) velocity in the beam and the dimensions of the loop. The observed linewidth at this time was 25 kc/sec. It seems most likely that the excess of observed over indirectly deduced (intrinsic) linewidths is due to slight static-field inhomogeneities.

The predictions of Hack's theory with respect to optimum rf power for a multiple quantum transition are thus well verified. An estimate of $\delta'\nu$ for potassium has been obtained by combining the theory and the potassium observations; and the potassium results may be used to provide a calibration of rf power indicators in terms of rf field in the transition region.

To apply these results to beams of other elements, we must provide for the possibility that they may have most probable speeds, hence $\delta'\nu$ values, different from that of the potassium beam. The desired relation is provided by the fact that a given atom orbit through the machine is characterized by $\mu H/Mv^2$, where μ is the high-field moment, $-g_J m_J \mu_0$, H is some fixed fraction of the maximum value of the A and B focusing fields, and M is the mass of the atom. Because $\delta'\nu \propto v$, we then have the proportion

$$\frac{\delta'\nu(X)}{\delta'\nu(\text{K})}=\left[\frac{m_J(X)}{m_J(\text{K})}\frac{g_J(X)}{g_J(\text{K})}\frac{M(\text{K})}{M(X)}\right]^{\frac{1}{2}}. \tag{16}$$

For arsenic $g_J\approx 2$, as for potassium; m_J, which is $\frac{1}{2}$ for focused potassium atoms, has the values $\frac{3}{2}$ and $\frac{1}{2}$ for arsenic. Thus, from the observed value of 13 kc/sec for potassium, we calculate values of 16 and 9 kc/sec for $\delta'\nu$ in the arsenic states $m_J=\frac{3}{2}$ and $\frac{1}{2}$, respectively.

We are now able to calculate optimum values of H_0 for the various arsenic multiple-quantum transitions from Eq. (15). These values, in absolute units, can then be converted to arbitrary units as indicated above. The results [obtained by use of first-order perturbed wave functions in Eq. (14)] are shown in Figs. 2 and 3, in which the tabulated unit is V^2. This is the square of an arbitrary unit, the voltage at the input to the rf loop, which is proportional to H_0, Thus, V^2 is proportional to the optimum rf power for the indicated transition.

EXPERIMENTAL RESULTS

Determination of the Spin of As^{76}

Using the apparatus and techniques described above, hfs resonances were observed in As^{76} at several values of static field up to about 5 oe. Some of these are shown in Figs. 5, 6, and 7. The counting rates involved were in the neighborhood of 3000 cpm; with 5-min counts the probable errors in relative intensity were somewhat less than 1% as indicated by the error flags.

Figure 5 shows a scan taken at a low field at the frequencies at which one would expect the resonances associated with transitions within the $F=\frac{5}{2}$ and $F=\frac{7}{2}$ states for $J=\frac{3}{2}$, $I=2$; these frequencies, calculated from Eq. (9) with the assumption that $g_J=2$, are indicated by arrows and the symbol ν_{lin}.

In the vicinity of the $F=\frac{7}{2}$ frequency, data were taken

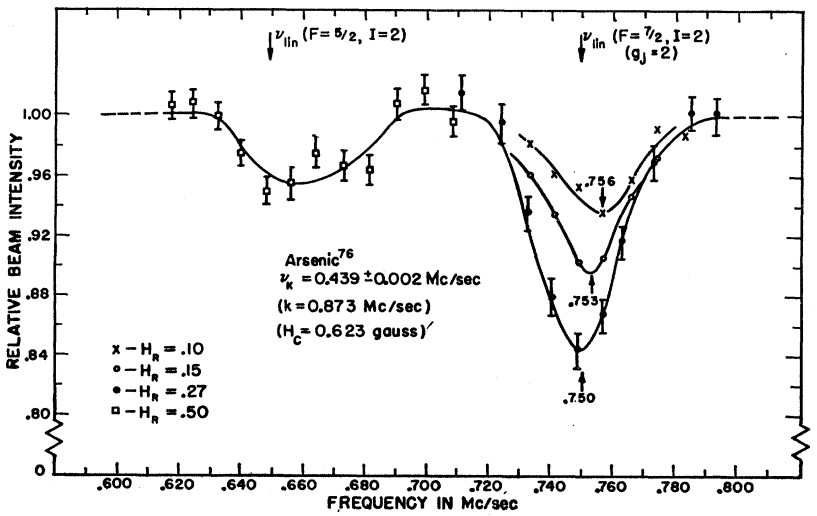

FIG. 5. Hyperfine structure transitions in $F=\frac{5}{2}$ and $F=\frac{7}{2}$ states of As^{76}. Positions of resonances predicted under assumptions that $I=2$, $g_J\approx 2$, and multiple quantum splitting unresolved at this value of field, are indicated by arrows. Shift of $F=\frac{7}{2}$ resonance to lower frequency as rf amplitude (H_R) is increased is ascribed to increasing influence of higher multiplicity transitions; see Fig. 2.

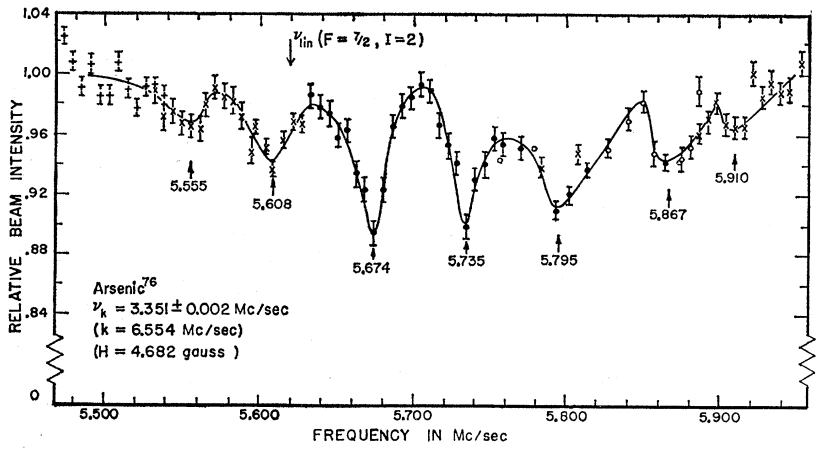

FIG. 6. Multiple quantum spectrum observed among the $F=\frac{7}{2}$ levels of As^{76} in a static field of 4.682 oe. The data were taken in four different runs, hence, the different symbols. The large arrow indicates the position of the transition occurring at the frequency ν_{1in} (i.e., dependent only to first order on the static field) predicted on the assumption that $I=2$ and $g_J=2$. One value of rf power ($V^2=100$ in terminology of text) used throughout.

at three different rf powers, as indicated in the figure; it is seen that the resonance shifts to lower frequencies as power is increased. This is to be expected in consequence of the increasing relative intensity, at higher powers, of the higher quantum-multiplicity transitions; increasing quantum multiplicity is associated with a decrease in resonance frequency to approximately ν_{1in} as shown in Fig. 2. At the value of the static field used here, the several multiple quantum transitions are not resolved.

The $F=\frac{7}{2}$ resonance was also observed at 1.482 Mc/sec at a static field of 1.223 oe (ν_{1in} calculated, as above, to be 1.468 Mc/sec, suggesting that quadratic terms are now beginning to enter).

We note at this stage that the assignment $I=2$ is already strongly indicated. The most nearly tolerable alternative would be $I=3$; for this assignment the two resonances just ascribed to $F=\frac{7}{2}$ would correspond to $F=9/2$. The corresponding values of ν_{1in} would be 0.585 Mc/sec and 1.142 Mc/sec; the two resonances of Fig. 5 would have to be adjacent multiple quantum resonances, both associated with $F=9/2$, and to give this large a multiple-quantum splitting (approximately 100 kc/sec) in the indicated static field, one would require the zero-field splitting $\Delta\nu_{9/2,7/2}$ to have a value of approximately 5 Mc/sec. This value would be surprisingly small; nevertheless, $I=3$ is not absolutely excluded by the data so far discussed.

The extensive data of Figs. 6 and 7 which correspond to the frequencies for $\Delta F=0$ transitions for $F=\frac{7}{2}$ and $\frac{5}{2}$, respectively, were taken at static fields of 4.682 and 1.540 oe, respectively, at which the multiple quantum resonances are found to be resolved. We note immediately that the data of either of these figures confirm the assignment $I=2$. The existence of a more or less uniform multiple-quantum splitting of about 60 kc/sec in Fig. 6 would not be possible at this field if $I=3$; for as just seen, if $I=3$, then $\delta\nu\approx 100$ kc/sec for $F=9/2$ at a static field of 0.6 guass (Fig. 5) and from this one would deduce $\delta\nu\approx 6000$ kc/sec [$\delta\nu\propto Hc^2$; see Eq. (12)], or 100 times the observed splitting at a static field of 4.7 oe (Fig. 6).

Detailed Multiple-Quantum Spectra for $F=\frac{5}{2}$ and $F=\frac{7}{2}$

Deductions of g_J and of the hyperfine structure intervals $\Delta\nu_{7/2,\frac{5}{2}}$ and $\Delta\nu_{\frac{5}{2},\frac{3}{2}}$ from the data require a more detailed analysis of Figs. 6 and 7. The intervals can be obtained from the experimental values of the multiple quantum-splittings $\delta\nu$, and Eq. (12). We note that $\Delta\nu_{7/2,\frac{5}{2}}$ can be determined from the data of the $F=\frac{7}{2}$ resonances alone. However, to obtain $\Delta\nu_{\frac{5}{2},\frac{3}{2}}$ (both intervals are necessary to calculate A and B; see below), data from the $F=\frac{5}{2}$ resonances are also required. Observation of the latter resonances was more difficult and the resulting data much less good than for $F=\frac{7}{2}$. The basic reasons for this relate to the strong-field atomic moments associated with the $F=\frac{5}{2}$ states, and to related questions of atom optics. From Fig. 1 it will be seen that the $F=\frac{7}{2}$ states have strong-field moments $3\,\mu_0$, μ_0, $-\mu_0$, $-3\,\mu_0$, whereas for $F=\frac{5}{2}$ the only moments are $\pm 3\,\mu_0$, $\pm\mu_0$, and $\mp\mu_0$ for $A<0$ or $A>0$. Thus, for the central five $\Delta F=0$ transitions for $F=\frac{7}{2}$, one sees that at sufficient multiple-quantum power m_J changes from $+\frac{3}{2}$ to $-\frac{3}{2}$, or the moment from $-3\,\mu_0$ to $+3\,\mu_0$, giving maximum flop-out effect. But for $F=\frac{5}{2}$ there are available no transitions for which the moment changes from $-3\,\mu_0$ to $+3\,\mu_0$. The $F=\frac{5}{2}$ resonances are therefore expected to be less intense than for $F=\frac{7}{2}$; in Fig. 5 the difference is a factor of 3.

For the resonances with less than maximum moment change, there will enter to some degree an effect observed[16] with rubidium in this apparatus (adjusted for flop-out operation). For Rb^{85} (because of its large $\Delta\nu$) some atoms make transitions between states with A-magnet moment $-\mu_0$ and B-magnet moment in the range $-0.3\,\mu_0$ to $-0.7\,\mu_0$; the result is observed to be a small signal which may be either flop-in or flop-out and

[16] O. Ames, A. Bernstein, and W. M. Hooke (private communication).

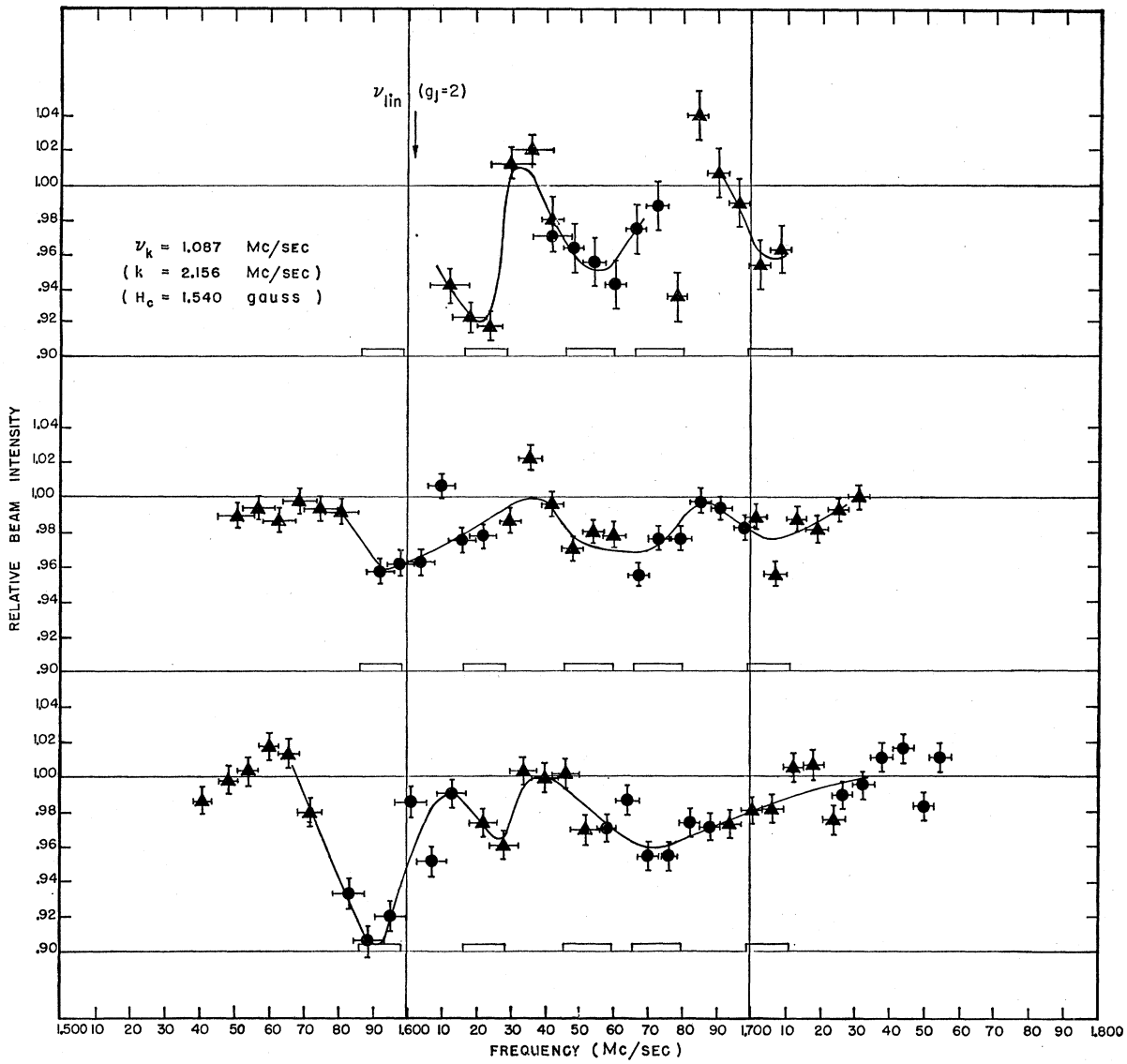

FIG. 7. Three separate runs through the $F=\frac{5}{2}$ multiple quantum spectra at a static field of 1.540 oe, with rf power parameter at 0.115 v^2. Boxes along horizontal axes indicate locations and uncertainties of resonance frequencies suggested by all three runs. Arrow again indicates expected position of ν_{lin} transition if $I=2$ and $g_J=2$. Different symbols for datum points serve merely to differentiate between disks used to collect the beam.

which is very sensitive to alignment. (This effect can be understood in terms of atoms which are brought to a focus *before* they reach the detector.) For $J=\frac{1}{2}$ (e.g., rubidium) such relative moment changes occur only for a few combinations of $\Delta\nu$ and of A- and B-magnet strength; but for $J\geq\frac{3}{2}$ (i.e., arsenic), they are common. Thus the $F=\frac{5}{2}$ resonances and the other $F=\frac{7}{2}$ resonances are expected, by comparison with the five central $F=\frac{7}{2}$ resonances, to be weaker and (because of alignment sensitivity) to be less reproducible.

The points just made are borne out by a comparison of the $F=\frac{7}{2}$ resonances (Fig. 6) and the $F=\frac{5}{2}$ resonances (Fig. 7). For $F=\frac{7}{2}$, resonances are seen at the following frequencies (in Mc/sec) at a static field of 4.682 oe:

5.555±0.005,	5.795±0.007,
5.608±0.005,	5.867±0.007,
5.674±0.004,	5.910±0.007.
5.735±0.004,	

For $F=\frac{5}{2}$ three runs, each taken at 1.540 oe, are shown separately; on the 0.90 relative intensity base line for each run the horizontal boxes indicate the frequency ranges which correspond to each of five resonances the presence of which is suggested by the data, as

follows (in Mc/sec):

1.593 ± 0.006, 1.673 ± 0.007,
1.622 ± 0.006, 1.705 ± 0.006.
1.653 ± 0.007,

It is apparent, however, that without great difficulty one could regard Fig. 7 as representing four resonances, say at frequencies 1.593, 1.622, 1.663, and 1.705 Mc/sec. The effects of this possibility are included in the subsequent discussion.

Identification of ν_{lin} and Determination of g_J

The procedure for interpretation of the multiple quantum data is to match the observed spectra of Figs. 6 and 7 with the predictions contained in their theoretical counterparts, Figs. 2 and 3. Strictly speaking, this would involve a process of successive approximation because the corrections (for third-order perturbation and frequency pulling) to the observed frequencies depend on the identification of individual resonances. However, such corrections are not large enough to change the matching of observed with theoretical spectra. We note that such matching supplies the conclusive evidence that the spin of As^{76} is 2.

The first step in interpretation of the data is to determine which of the empirical resonances in each spectrum corresponds to ν_{lin}. This will provide an origin from which the other resonances may be identified. We note, however, from Figs. 2 and 3, that most observed resonances may consist of two multiple quantum transitions (even three for $F=\frac{7}{2}$, $A>0$ if $m_J=\frac{3}{2}\rightarrow\frac{1}{2}$ transitions are observable). Thus, the relative weights of each transition need to be considered. This is dealt with below, but has only insignificant effect on our determination of ν_{lin}.

Another important consequence of a measurement of ν_{lin} is the fact that this yields directly the value of g_J; see Eq. (9).

A comparison of theory (Fig. 2) and experiment (Fig. 6) for $F=\frac{7}{2}$ shows that the applied rf power ($V^2=100$ v^2) is sufficient to excite at least one of the contributing transitions at the frequency of each multiple quantum resonance; and since seven resonances are observed, ν_{lin} must be one of the three lowest frequency resonances in Fig. 6. For $\nu_{\text{lin}}=5.555$, 5.608, and 5.674, with probable errors as stated above and with corrections for third order and pulling as indicated in Fig. 2, the corresponding values of g_J are 1.977 ± 0.002, 1.996 ± 0.002, 2.020 ± 0.002. For $F=\frac{5}{2}$ the applied rf power ($V^2=0.115$ v^2) is not sufficient to excite the predicted four-quantum resonance of lowest frequency. As shown in the previous discussion [see Eq. (13)], the transition probability for grossly underpowered N-quantum transitions is proportional to (applied power/optimum power)^N. A detailed analysis shows that at $V^2=0.115$ v^2, the lowest frequency transition in question has transition probability well below 10^{-2}. Thus, a comparison of theory (Fig. 3) and experiment (Fig. 7) shows that in the five-resonance interpretation of Fig. 7 we must have $A<0$ and that the lowest observed frequency is ν_{lin}, corrected as indicated in Fig. 3 to 1.594 ± 0.003 Mc/sec; this gives $g_J=1.990\pm0.004$. On the four-resonance interpretation, ν_{lin} is either the lowest observed frequency (again, $g_J=1.990\pm0.004$) or a diatance $\delta\nu$ below the lowest frequency; if $\delta\nu$ is taken to be 29 ± 3 kc/sec, this latter alternative gives $g_J=1.954\pm0.006$.

The assignments of ν_{lin} in the $F=\frac{5}{2}$ and $F=\frac{7}{2}$ spectra must, of course, be consistent with each other. It is seen from the above that the only possible value of g_J which is consistent with both these spectra is

$$g_J=1.994\pm0.003,$$

and that ν_{lin} is the second lowest frequency resonance in the $F=\frac{7}{2}$ spectrum and the lowest for the $F=\frac{5}{2}$ spectrum. It will be noted that this value of g_J does not depend on a choice between the four-resonance or the five-resonance interpretation of Fig. 7 and is consistent with either sign of A. It should also be noted that the theoretical frequency pulling by the rf power is so small that if this frequency pulling were to be ignored completely the above value of g_J would not be changed.

It should finally be noted that the optimum power calculation is not an irreplaceable step in the deduction of the above g_J. Without the optimum power calculation, one would be forced to consider the following possibility: $A>0$, ν_{lin} the second lowest resonance for $F=\frac{5}{2}$ and third lowest for $F=\frac{7}{2}$, $g_J=2.021\pm0.002$. But this interpretation is untenable for two reasons, aside from optimum power considerations: first, it requires that the m_J transition $\frac{1}{2}\rightarrow-\frac{3}{2}$ be invisible and $\frac{1}{2}\rightarrow-\frac{1}{2}$ be visible, which is completely unreasonable as a matter of atom optics. Second, and most conclusively, in the $F=\frac{7}{2}$ Zeeman resonance of Fig. 5, this g_J would give $\nu_{\text{lin}}=0.756$ Mc/sec which is not consistent with the deduction from this figure that $\nu_{\text{lin}}\leq0.750$ Mc/sec.

In our derivation of the expression for multiple-quantum resonance frequencies in general and for ν_{lin} in particular, we have omitted terms in g_I. This omission leads to a fractional inaccuracy in our value of g_J roughly equal to the ratio g_I/g_J. However, from the known value[3] of g_I this is found to be about one-tenth the fractional uncertainty we quote above for g_J; hence, our neglect of g_I is justified.

Relative Frequency Pulling of Transitions

In theory,[15] frequency pulling is proportional to rf power. The rf power used in obtaining the $F=\frac{7}{2}$ data of Fig. 6 ($V^2=100$ v^2) was optimum for a six-quantum transition; correspondingly, the calculated pulling indicated in Fig. 2 for the low-multiplicity transitions is much greater than for those with $N\geq4$, for which it

is at most several kc/sec. As Kusch[17] has shown, theoretical calculations of frequency pulling and of linewidth cannot be relied on in the case of gross overpowering of a transition; and the actual pulling is sensitive to the geometry of the rf field. He has also shown that, at optimum power for a high-multiplicity transition, the linewidth increases when one examines transitions of lower multiplicity, although, again, the variation is not as marked as theory predicts. The qualitative conclusions, however, are clear: at optimum power for six-quantum transitions, as used in Fig. 6, the predictions in Fig. 2 of the not over several-kilocycles-frequency pulling for $N\geq 4$ should be reliable at least to better than a kilocycle; the predicted larger frequency pullings for $N=1, 2, 3$ are not to be trusted in quantitative detail. Also, the lower the quantum multiplicity of a given transition, the broader the resonance. For $F=\frac{7}{2}$, we shall therefore draw quantitative conclusions concerning frequencies from only the four lowest frequency (i.e., highest multiplicity) resonances.

For the $F=\frac{5}{2}$ resonances (Fig. 7) the applied rf power ($V^2=0.115$ v^2) was much lower than for $F=\frac{7}{2}$, being slightly less than the optimum for $N=3$ at this frequency. The calculated frequency pulling is small and represents no significant problems for $F=\frac{5}{2}$.

Determination of $\delta\nu_{7/2}$ and $\delta\nu_{\frac{5}{2}}$

We have thus concluded that for $F=\frac{7}{2}$ we shall draw quantitative frequency conclusions from the four lowest frequency resonances. We now note further that consideration of the relative intensity of the several components of these resonances, as given in the Appendix, indicates that we should ascribe to the strongest associated component the frequency of the observed resonance. Correspondingly, we use for each resonance the correction for theoretical frequency pulling and third-order shift which, according to the Appendix, is associated in Fig. 2 with the strongest component. Thus, we have for the relevant second-order frequencies of the $F=\frac{7}{2}$ spectrum: 5.555 ± 0.005, $5.608\pm0.005(=\nu_{1\text{in}})$, 5.673 ± 0.004, 5.736 ± 0.004 Mc/sec, giving for $\delta\nu_{7/2}$ the three respective differences 53 ± 7, 65 ± 7, and 63 ± 6 kc/sec. Taking one-third the splitting of the extremes, we have finally

$$\delta\nu_{7/2}=60\pm2 \text{ kc/sec}.$$

The determination of $\delta\nu_{\frac{5}{2}}$ is made relatively imprecise by the scatter among the data of Fig. 7. The separation of the first two resonances gives $\delta\nu_{\frac{5}{2}}\approx 29\pm6$ kc/sec. A four-resonance interpretation in which one interprets the nominal third and fourth resonances as a single one gives $\delta\nu_{\frac{5}{2}}\approx 37\pm3$ kc/sec. Finally, we take an all-inclusive value

$$\delta\nu_{\frac{5}{2}}=31\pm9 \text{ kc/sec}.$$

with which is associated a value of $\nu_{1\text{in}}$ of 1.593 Mc/sec.

[17] P. Kusch, Phys. Rev. **101**, 627 (1956).

Not only is the magnitude of the $\delta\nu$'s significant, but so is the sign, as shown in the next section. The positive signs follow from the definition of $\delta\nu$ and the observation that the multiple-quantum spectra extend from $\nu_{1\text{in}}$ towards higher frequencies.

INTERPRETATION OF RESULTS

Shell Model Considerations of Spin

The first result of this experiment is a determination that the spin of As^{76} is 2. Beta decay systematics[18] have indicated a spin-parity assignment of 2−. This value of spin agrees with a simple prediction of the nuclear shell model. Arsenic has 33 protons. In the region from $Z=28$ to 38 there is competition between $p_{\frac{3}{2}}$ and $f_{\frac{5}{2}}$ levels for the ground state. The fact that such nuclei with odd mass usually are in the $p_{\frac{3}{2}}$ state (As^{75} is in this category) is ascribed to a "pairing energy" which tends to cause nucleons to fill the $f_{\frac{5}{2}}$ level in pairs, permitting the odd proton to be in the $p_{\frac{3}{2}}$ state. The same effect obtains in the case of odd-neutron nuclei with N between 38 and 50, except here the competition is between $p_{\frac{1}{2}}$ and $g_{9/2}$ levels. The measured spins of odd-neutron, even-proton nuclei in this region indicate that the competition is quite close.

Of the four possible combinations of the two proton and two neutron states in question, $(\pi f_{\frac{5}{2}})$ $(\nu g_{9/2})$ is chosen as the most likely odd proton, odd neutron configuration. This is the only one of the four which agrees with Nordheim's rules[19] in giving a spin of 2. However, the observed[3] magnetic moment, $-0.90\,\mu_N$, does not agree with the value ($\mu_{\text{calc}}=-1.43\,\mu_N$) associated with this assignment using empirical neutron and proton moments from adjacent nuclei.

The most plausible shell-model state which has the correct spin and parity and which, if mixed with the above state, would provide a fit to the magnetic moment, is[20] $(\pi f_{\frac{5}{2}})(\nu g_{9/2}{}^3)_{7/2}$ ($\mu_{\text{calc}}=-0.52\,\mu_N$).

Hfs Intervals and Constants

Having determined the second-order multiple quantum frequency intervals, $\delta\nu$, above, we can now determine the two uppermost zero-field hfs intervals, $\Delta\nu_{7/2,\frac{5}{2}}$ and $\Delta\nu_{\frac{5}{2},\frac{3}{2}}$, by means of Eq. (12). It is to be emphasized that the values of $\delta\nu$ obtained above have already been corrected for third-order terms, so we neglect the last term in the cited equation.

For the $F=\frac{7}{2}$ spectrum, Eq. (12) simplifies to

$$\Delta\nu_{7/2,\frac{5}{2}}=\pm(2/9)\nu_{1\text{in}}{}^2(\delta\nu_{7/2})^{-1}. \quad (17)$$

[18] J. D. Kurbatov, B. B. Murray, and M. Sakai, Phys. Rev. **98**, 674 (1955); F. T. Kokoszka, D. R. Cartwright, and J. D. Kurbatov, Bull. Am. Phys. Soc. **3**, 207 (1958).

[19] L. A. Nordheim, Revs. Modern Phys. **23**, 322 (1951).

[20] A. M. Bernstein (private communication), see also M. H. Brennan and A. M. Bernstein, Phys. Rev. **120**, 927 (1960).

Similarly, for the $F=\frac{5}{2}$ spectrum, we have

$$\Delta\nu_{\frac{5}{2},\frac{3}{2}}=\pm\frac{343}{338}\left(\frac{\delta\nu_{\frac{5}{2}}}{\nu_{1\mathrm{in}}{}^2}+\frac{50}{169}\frac{1}{|\Delta\nu_{7/2,\frac{5}{2}}|}\right)^{-1}. \quad (18)$$

Inserting the measured $\delta\nu$'s and $\nu_{1\mathrm{in}}$'s gives

$$\Delta\nu_{7/2,\frac{5}{2}}=\pm(117\pm4)\text{ Mc/sec},$$
$$\Delta\nu_{\frac{5}{2},\frac{3}{2}}=\pm(69\pm16)\text{ Mc/sec}.$$

In the foregoing, the sign is to be chosen to agree with that of A. Thus, we have not determined whether the hfs is "normal" or "inverted," but only that the energy levels $F=\frac{7}{2}$, $\frac{5}{2}$, $\frac{3}{2}$ are in monotonic order, either from higher to lower energies or vice versa.

The intervals between the $F=\frac{7}{2}$, $\frac{5}{2}$, and $\frac{3}{2}$ levels are related to A and B as shown in Eqs. (3) which are solved to give

$$A=\pm(30.5\pm3.5)\text{ Mc/sec},$$
$$B=\pm(12\pm14)\text{ Mc/sec}.$$

Magnetic Field at Arsenic Nucleus

In principle it is possible to calculate the value of $H(0)$ from various atomic spectroscopic data by the techniques described by Breit and Wills.[21] This would permit determination of μ_I from A via Eq. (1). However, it turns out that we cannot rely on this approach to calculate the magnetic interaction for this atom. For example, a straightforward application of the theory does not agree with experiment in the case of the similar atom Bi^{209}. There, simple theory predicts A and μ_I to have the same sign, whereas it has been observed that A is negative[22] and μ_I positive.[23] One cause of this discrepancy is the assumptions which must be made about the contribution of each valence (p) electron when in either of the states $j=\frac{3}{2}$ or $\frac{1}{2}$. A more refined, phenomenological estimate of these contributions was made for this atom by Breit and Wills by means of Goudsmit's sum rule. This approach is not feasible for As because the required input data (the values of A in the $^2D_{\frac{5}{2}}$ and $^2P_{\frac{3}{2}}$ terms arising from the same configuration) are not available.

One important origin of the hfs interaction in these $^4S_{\frac{3}{2}}$ atoms, hence of the discrepancy between experiment and the cited theory which does not consider this point, is configuration interaction. The ground state configuration of As is $4s^24p^3$; the paired s electrons contribute nothing to the hfs. However, unpaired s electrons, because of their close approach to the nucleus, contribute strongly to this interaction, i.e., produce a large magnetic field at the nucleus. From parity considerations, the most probable configuration to be so considered is $4s4p^35s$. From Kopfermann's[13] Sec. 26 (and using the energy levels for As given in the NBS Tables) we may derive the a values for those two s electrons: $a_{4s}\approx300$ Mc/sec; $a_{5s}\approx100$ Mc/sec. Thus, only a small admixture of that configuration is needed to contribute sufficient field to produce the value of A we have observed.

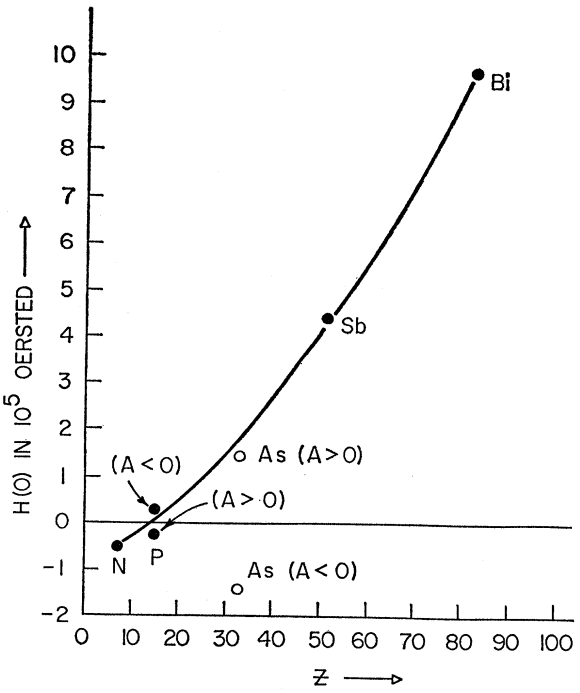

FIG. 8. Magnetic field at nucleus for atoms of column 5-A of periodic table calculated from nuclear spins and moments and magnetic hfs interaction constants as described in text. Sign of H is relative to that of J; single electron atoms have $H<0$. Signs of hfs interactions in phosphorous and arsenic have not yet been determined; a smooth variation requires that A be positive for the latter.

From the available spectroscopic information we are not able to calculate $H(0)$; thus, we cannot calculate μ_I from A. Furthermore, A has not been measured for the ground state of the stable isotope (As^{75}) (but see below) which precludes a Fermi-Segrè comparison[1] of moments and hfs intervals. However, we may work backwards, using the value of $\mu_I=-0.9028(\pm0.005)\mu_N$ recently determined for As^{76} by Pipkin and Culvahouse,[3] and our value of A, to determine $H(0)$ from Eq. (1):

$$H(0)=\pm(1.33\pm0.15)\times10^5\text{ oe}.$$

Optical hfs spectroscopy of As^{75} by Hults and Mrozowski[24] has indicated that the total splitting in the ground state is about 0.010 or 0.015 cm^{-1}. This corresponds to A_{75} of about 50 to 75 Mc/sec and thus, $H(0)$ of about 1.0 to 1.5×10^5 oe in excellent agreement with the above magnitude.

It is interesting to calculate $H(0)$ for the other atoms of this column of the periodic table. This we have done, using the data of the following references: N^{14} [25]; P^{31} [26];

[21] G. Breit and L. A. Wills, Phys. Rev. **44**, 470 (1933).
[22] S. Mrozowski, Phys. Rev. **62**, 526 (1942).
[23] W. G. Proctor and F. C. Yu, Phys. Rev. **78**, 471 (1950).
[24] S. Mrozowski (private communication).
[25] L. W. Anderson, F. M. Pipkin, and J. C. Baird, Phys. Rev. **116**, 87 (1959).
[26] H. G. Dehmelt, Phys. Rev. **99**, 527 (1954).

TABLE I. Measured values of g_J for atoms of column 5-A elements.

Atom	g_J	References
N	2.0021	a
P	2.0019	b
As	1.994	this paper
Sb	1.9705	c
Bi	1.6433	d

[a] M. A. Heald and R. Beringer, Phys. Rev. **96**, 645 (1954).
[b] H. G. Dehmelt, Phys. Rev. **99**, 527 (1954).
[c] P. C. B. Fernando, G. K. Rochester, I. J. Spalding, and K. F. Smith, Phil. Mag. **5**, 1291 (1960).
[d] R. S. Title and K. F. Smith, Phil. Mag. **5**, 1281 (1960).

Sb^{121} [27]; Bi^{209} [22,28] The results are shown in Fig. 8. A smooth variation of $H(0)$ with atomic number Z is indicated, regardless of the sign of A in phosphorus, but providing A is positive for As^{76}.

Relation between B and Q

The electric quadrupole moment of the As^{76} nucleus can be determined from B by means of Eq. (2) if the factor q is calculated. (From our value of B only an upper limit can be placed on the magnitude of Q.) That factor is given by[18]

$$q=-e\langle r^{-3}(3\cos^2\theta-1)\rangle_{JJ},$$

where the subscripts indicate the expectation value of the indicated electron coordinates is to be taken over the state $J=\frac{3}{2}=m_J$. This expectation value is calculated for our p^3 configuration as shown by Schüler and Schmidt[29] with intermediate coupling wave functions.[21,30] The result is that for the ground state of atomic arsenic,

$$Q(\text{barn})=-0.58B(\text{Mc/sec}). \quad (19)$$

Our measured value of B therefore indicates

$$Q_{76}=\mp(7\pm8)\text{ barn}.$$

Comparison of g_J-Values of Column 5-A Atoms

We have previously indicated that the value of g_J for As is 1.994 ± 0.003. This agrees reasonably with a value calculated by Inglis and Johnson[31] of 1.988. There are now measured values of g_J for all the atoms in column 5-A of the periodic table; these are shown in Table I. The monotonic decrease in g_J values from lighter to heavier atoms is in agreement with the well-known trend from LS coupling toward jj coupling. The p^3 electron configuration of these atoms has a ground S state in pure LS coupling, which would be expected to have the g_J value of a single s electron, 2.0023. In the other extreme (pure jj coupling), the g_J value would be 1.333.

Trees[32] has shown that in the case of nonrelativistic LS coupling there is no hfs for S states not made up of s electrons. The apparent slight deviation of As away from pure LS coupling, evidenced by the g_J value, correlates with the presence of nonzero but modest values for the hfs energy separations found in this experiment.

ACKNOWLEDGMENTS

We are indebted to Drs. O. Ames, A. M. Bernstein, and W. M. Hooke for assistance with the "$F=\frac{5}{2}$" part of this experiment.

APPENDIX

At the values of external field of Figs. 6 and 7, a given resonance has, in general, several components, i.e., corresponds to several different transitions at closely the same frequency, differing in fact only by the third-order and pulling effects. We here consider the question, "What is the relative intensity of these several components of a given resonance?," in order to apply the appropriate frequency corrections for pulling and third-order shift to each experimental resonance.

We note first of all by comparison with Fig. 2 that no resonance in Fig. 6 can correspond to more than two transitions. If transitions between states with $m_J=\frac{3}{2}$ and $\frac{1}{2}$ were observable (as is not expected) and if A were positive we could have three transitions for certain resonances; but this probability is eliminated by the absence of a resonance at $(\nu_{1\text{in}}-2\delta\nu)$.

Also from Fig. 2, we note that at optimum power for $N=6$, the one $N=7$ transition is underpowered by a factor of 2.2; but any deductions of exact reduction in intensity from this fact alone will be very sensitive to velocity-distribution assumptions and had best be avoided.

Further conclusions concerning the relative weight of the transitions which are listed in Fig. 2 must depend on a detailed analysis of the intensities of the observed resonances, and this analysis depends in turn on an assumption concerning the effect of overpowering on intensity. For this purpose we assume the overpowered transition to have an intensity (0.6 ± 0.1) times the optimum-powered transition. The deduction of this factor has two ingredients. The first is 0.5 (the average of a sine-squared transition probability), which for a beam of any velocity distribution having nonzero velocity spread should give the reduction for a grossly overpowered resonance as compared to the same resonance when optimum-powered for a monoenergetic beam. The second is 0.7 which gives the reduction in going, at optimum power, from a monoenergetic to a Maxwellian velocity distribution. Thus, for a grossly overpowered resonance as compared to an optimum-powered one, the reduction factor should lie between $0.5/0.7=0.7$ for a Maxwellian distribution and 0.5/1

[27] P. C. B. Fernando, G. K. Rochester, I. J. Spalding, and K. F. Smith, Phil. Mag. **5**, 1291 (1960).
[28] R. S. Title and K. F. Smith, Phil. Mag. **5**, 1281 (1960).
[29] H. Schüler and T. Schmidt, Z. Physik **99**, 717 (1936).
[30] D. R. Inglis, Phys. Rev. **38**, 862 (1931).
[31] D. R. Inglis and M. H. Johnson, Jr., Phys. Rev. **38**, 1642 (1931).
[32] R. E. Trees, Phys. Rev. **92**, 308 (1953).

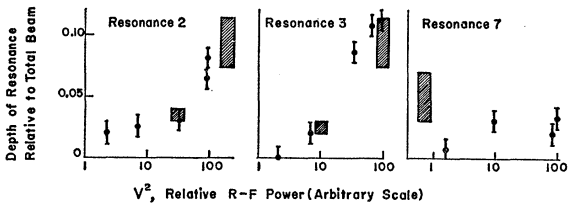

FIG. 9. Relative depth of resonance as a function of rf power for three resonances (numbered from lower to higher frequency) of the $F=\frac{7}{2}$ spectrum, Fig. 6. Cross-hatched areas represent expected values based on assignment of m_J values as discussed in text. Points are experimental values, with their uncertainties.

$=0.5$ for a comparatively (but not completely) monoenergetic beam; hence, we use 0.6 ± 0.1.

We now summarize below the principal results of of this analysis of the observed resonances of Figs. 6 and 7. Here we denote by $D(m_J,m'_J)$ the depth of resonance of a given transition at optimum power; the $D(m_J,m'_J)$ depend primarily upon the velocity distribution provided by the microwave discharge source and upon the atom optics of the beam apparatus.

The $D(m_J,m'_J)$ are largest for the m_J transitions which correspond to reversal of sign, without change in magnitude, of the initial high-field moment. More specifically, we find $D(\frac{3}{2},-\frac{3}{2})=0.09\pm0.02$ and $D(\frac{1}{2},-\frac{1}{2})=0.10\pm0.03$. On the other hand, the m_J transitions $\frac{1}{2}$ to $-\frac{3}{2}$ and $\frac{3}{2}$ to $-\frac{1}{2}$ are comparatively weak; the deduced $D(m_J,m'_J)$ are slightly dependent on the sign of A and on which of the two m_J transitions is involved, but are in any case all included in the statement

$$D(\tfrac{1}{2},-\tfrac{3}{2})\approx D(\tfrac{3}{2},-\tfrac{1}{2})\approx 0.045\pm0.02.$$

Separate comment should be made concerning transitions between states having $m_J=\frac{1}{2}$ and $\frac{3}{2}$, which would be expected, from atom-optical considerations, to be even weaker than any of those discussed above. (Note that states with either $m_J=\frac{1}{2}$ to $\frac{3}{2}$ are focused; note further that a change of m_J either from $\frac{1}{2}$ to $\frac{3}{2}$ or from $\frac{3}{2}$ to $\frac{1}{2}$ could conceivably change the focused beam intensity and produce an observable result; hence, we have used in the preceding sentence the phrase "between $\frac{3}{2}$ and $\frac{1}{2}$" rather than the possibly expected "from $\frac{3}{2}$ to $\frac{1}{2}$".) If $A>0$ then, as already mentioned, the $\frac{3}{2}$ to $\frac{1}{2}$ transition at $(\nu_{1\text{in}}-2\delta\nu)$ in the $F=\frac{7}{2}$ spectrum indicates $D(\frac{3}{2},\frac{1}{2})=0$. If $A<0$ then a fifth resonance for $F=\frac{5}{2}$ could only be the $\frac{3}{2}$ to $\frac{1}{2}$ transition and conversely the existence of a fifth $F=\frac{5}{2}$ resonance, the suggestion of which in Fig. 7 has already been discussed, would prove $A<0$; but this is the only indication that $A<0$ and is not to be relied upon. If $A<0$, the one $\frac{3}{2}$ to $\frac{1}{2}$ transition in the $F=\frac{7}{2}$ spectrum should be so strongly pulled as not to have been seen.

TABLE II. Relative intensities of the two contributions, identified by (m_J,m'_J), which can make up the four resonances of Fig. 6 used to determine $\delta\nu$.

Resonance (Mc/sec)	Relative intensities $(\frac{3}{2},-\frac{1}{2})$ or $(\frac{1}{2},-\frac{3}{2})$	$(\frac{3}{2},-\frac{3}{2})$
5.555	1	0
5.608	0.3	0.7
5.674	0.2	0.8
5.735	0.4	0.6

The net result of the above anaylsis of $D(m_J,m'_J)$ factors is that the m_J transition $\frac{3}{2}$ to $-\frac{3}{2}$ (which cannot occur in the $F=\frac{5}{2}$ spectrum) predominates in the central five resonances of the $F=\frac{7}{2}$ spectrum, while $\frac{1}{2}$ to $-\frac{1}{2}$ (which in the $F=\frac{7}{2}$ spectrum is probably so strongly pulled as not to have been seen) predominates in the $F=\frac{5}{2}$ spectrum. In the $F=\frac{7}{2}$ spectrum the m_J transitions ($\frac{1}{2}$ to $-\frac{3}{2}$ and $\frac{3}{2}$ to $-\frac{1}{2}$ provide the two weak extreme-frequency resonances, numbers 1 and 7 (in order of increasing frequency), and make a minor contribution to resonances 2, 3, 4, 5. In the $F=\frac{5}{2}$ spectrum, because of the level of the applied rf power, these transitions should contribute only to a fourth resonance.

Experimental evidence which is in agreement with the results of the considerations concerning power dependence used in carrying out the above analysis is shown in Fig. 9. We note that the lowest-power point in resonance 7 could conceivably correspond to the minimum in transition probability which occurs for a velocity selected beam and a two-quantum transition (like this one) at twice optimum power. Aside from this one possibly anomalous point, the dependence of relative resonance depth on rf power is seen to agree well with the expected dependence.

We now use the above $D(m_J,m'_J)$, together with the assumed reduction factor of (0.6 ± 0.1) due to overpowering, to deduce the relative intensities given in Table II. for the various (m_J,m'_J) components of Fig. 6. In each of the three compound resonances given in Table II, the weaker component has the lower quantum multiplicity, hence a frequency width which is greater by an unknown amount of that of the strong component, and so an influence in locating the observed resonance which is even less than the weights listed above. All told, it seems best to ascribe the observed frequency to the strongest component of each resonance and to make corrections accordingly; this was the approach used in the body of this paper.